

From the second magnetization peak to peak effect. A study of superconducting properties in Nb films and MgB₂ bulk samples

Dimosthenis Stamopoulos,[‡] Athanasios Speliotis and Dimitris Niarchos

Institute of Materials Science, NCSR "Demokritos", 153-10, Aghia Paraskevi, Athens, Greece.

(Dated: September 4, 2018)

We report on magnetic and magnetoresistance measurements in two categories of superconducting Nb films grown via magnetron sputtering and MgB-2 bulk samples. In the first category, films of $T_c = 9.25$ K were produced by annealing during deposition. In these films, the magnetic measurements exhibited the so-called "second magnetization peak" ("SMP"), which is accompanied by thermomagnetic instabilities (TMI). The characteristic field H_{fj} , where the first flux jump occurs, has been studied as a function of the sweep rate of the magnetic field. Interestingly, in the regime $T < 6.4$ K, the respective line $H_{fj}(T)$ is constant, $H_{fj}(T < 6.4 \text{ K}) = 40$ Oe. A comparison to TMI observed in MgB₂ bulk samples is also performed. Our experimental findings can't be described accurately by current theories on TMI. In the second category, films of $T_c = 8.3$ K were produced without annealing during deposition. In such films, we observed a peak effect (PE). In high magnetic fields the PE is accompanied by a sharp drop and a narrow hysteretic behavior ($\Delta T < 20$ mK) in the measured magnetoresistance. In contrast to experimental works presented in the past, the comparison of our magnetic measurements with the magnetoresistance data suggests that rather the appearance of surface superconductivity than the melting transition of vortex matter, is the cause of the observed behavior.

PACS numbers: 74.78.Db, 74.25.Ha, 74.25.Fy, 74.25.Op

INTRODUCTION

The discovery of compounds that exhibit high critical temperatures opened a new wide field in the physics of superconductivity [1]. A consequence of the ongoing theoretical and experimental interest for the effects observed in high- T_c compounds, is the reexamination of the related topics in the more isotropic low- T_c superconductors [2, 3, 4]. Interestingly, current theoretical studies try to unify the phase diagram of vortex matter by appropriately taking into account all the factors that influence the behavior of the magnetic flux lines created in both low and high-temperature superconductors [2, 3].

Isotropic Nb is a low- T_c conventional superconductor which recently has become a subject of intensive experimental studies [5, 6, 7, 8, 9, 10, 11, 12, 13]. One of the unresolved issues is the nature of the vortex state which is settled in the regime close to the upper-critical field $H_{c2}(T)$. More specifically, questions on the importance of fluctuation effects [8] and the nature of the melting transition and/or an order-disorder transition is still under investigation in this type-II superconductor [9, 10, 11, 12, 13]. In addition, recent magnetic studies in Nb films [14, 15] reported the existence of a structure that reminisces of the second magnetization peak (SMP) which is usually observed in high- T_c superconductors [16, 17, 18, 19, 20]. These studies concluded that for the case of Nb films the "second magnetization peak" ("SMP") is motivated by thermomagnetic instabilities

(TMI) that occur in the low-temperature regime, far below the upper-critical field [14, 15, 21]. Despite the need for the complete theoretical understanding of the underlying mechanism that motivates the "SMP", the existence of the accompanying TMI should be studied experimentally in more detail, because the undesirable flux jumps constitute a serious limitation for practical applications. Finally, in the last years many experimental and theoretical works dealt with the change of the superconducting properties of Nb films, when placed in close proximity with arrays of ferromagnetic particles or magnetic homogenous layers [22, 23, 24, 25]. Such composite structures may constitute a starting point for the generation of important electronic devices in the near future [22]. Thus, thorough studies of the phase diagram of vortex matter in pure Nb, and other low- T_c superconducting films, may give information that could be important in other areas of science.

In spite of the ongoing experimental research, a complete study of the phase diagram of vortex matter in an extended temperature-magnetic-field regime is still lacking, leaving the above mentioned issues still open. To this end, we performed systematic magnetic and transport measurements in sputtered polycrystalline films of the low- T_c Nb superconductor. In relatively thick samples, *produced by annealing during the deposition*, the magnetic measurements exhibited a "SMP" at points $H''_{\text{smp}}(T)$, which is placed well below the upper-critical fields $H_{c2}(T)$. The "SMP" is accompanied by flux jumps, occurring for $H < H''_{\text{smp}}(T)$, while for $H > H''_{\text{smp}}(T)$ smooth $m(H)$ curves are observed. For low enough temperatures $T < 6.4$ K, the first flux jump line $H_{fj}(T)$, where the first flux jump in the virgin magnetic curve is

[‡]Corresponding author (densta@ims.demokritos.gr)

observed, becomes constant $H_{fj}(T < 6.4 \text{ K}) = 40 \text{ Oe}$. Furthermore, the characteristic field $H_{fj}(T)$ is not inversely proportional to the sweep rate of the applied field. These experimental findings are in strong contrast to theoretical expectations and remain to be explained. The first flux jump line $H_{fj}(T)$ ends at a characteristic temperature $T_o = 7.2 \text{ K}$, where it connects with the first peak $H_{fp}(T)$, and with the "SMP" $H''_{\text{smp}}(T)$ lines. For $T > T_o = 7.2 \text{ K}$ no flux jumps were observed, in nice agreement to theoretical suggestions. In order to compare the TMI observed in films and in bulk samples we also present supplementary magnetic data in a MgB_2 bulk sample. The comparison revealed many differences in the observed behaviors.

In thinner films, *produced without annealing during the deposition*, transport measurements revealed a conventional peak effect (PE), placed in the vicinity of the upper-critical fields $H_{c2}(T)$. For high enough magnetic fields, the response at the end points $H_{ep}(T)$ of the PE exhibits a narrow hysteretic behavior ($\Delta T < 20 \text{ mK}$). The hysteresis fades as we move in the low-field regime. In addition, the hysteretic response is current dependent (not observed in very small or high currents), indicating that is motivated by a dynamic cause. A discussion referring to surface superconductivity and to the melting and/or disordering transition of vortex matter in Nb is made.

This paper is organized as follows. In Sec. II we give details about the preparation of the films and the performed experiments. Section III presents magnetic and transport data for the film Nb-1 that exhibits the "SMP" and the TMI. The vortex matter phase diagram is constructed, and a discussion is made in comparison to current theories on TMI. A brief comparison with recent magneto-optical studies in Nb and MgB_2 films is also made. In Sec. IV we present experimental results for the film Nb-2 that exhibits the PE. The phase diagram of vortex matter for the Nb-2 sample is also presented. An extended discussion on the disordering and the melting transitions, and also on surface superconductivity is made. In Sec. V we present crystallographic results coming from transmission electron microscopy (TEM) and x-ray diffraction (XRD) experiments and we make a comparative discussion on the results that the two different films exhibit. Finally, the conclusions are presented in Sec. VI.

PREPARATION OF THE FILMS AND EXPERIMENTAL DETAILS

The samples of Nb were sputtered on Si [001] substrates under an Ar atmosphere (99.999 % pure). The base pressure was $5 \times 10^{-7} \text{ Torr}$. We examined in detail the influence of the deposition rate and of the annealing temperature (during the deposition) on the quality

of the produced films. As a criterion, we measured the upper-critical field line $H_{c2}(T) = \Phi_o/2\pi\xi^2(T)$ of the produced Nb films. The films that were produced at deposition rates of the order of 4 \AA/sec (at a DC power of 55 Watt) exhibited the smallest slope $dH_{c2}(T)/dT$. In this work we present data on two categories of sputtered films. The first category refers to films produced by annealing at $T = 300 \text{ C}$ during deposition. Such films exhibit a critical temperature 9.25 K , equal to the one of high purity single crystals [26]. The second category refers to films produced without annealing during the deposition. These films showed a critical temperature of 8.3 K . Below we present results for a representative Nb film of each category. The Nb film of the first category is labelled as Nb-1 and has $T_c = 9.25 \text{ K}$, while the one of the second category is labelled as Nb-2 and has $T_c = 8.3 \text{ K}$. The residual resistance ratio was $R(300 \text{ K})/R(10 \text{ K}) = 6.8$ and 2.9 for Nb-1 and Nb-2 respectively. Their thickness is 7700 \AA and 1600 \AA for Nb-1 and Nb-2 respectively.

Our magnetic measurements were performed by means of a commercial SQUID magnetometer (Quantum Design). In all magnetic data presented below, the magnetic field was always normal to the surface of the film ($\mathbf{H} \parallel \mathbf{c}$). All the magnetization data were obtained under zero field cooling (ZFC). In this experimental protocol, by starting from a temperature above T_c , the sample is cooled to the desired temperature under zero magnetic field. In this way, we obtain the virgin magnetization curves. Our magnetoresistance measurements were performed by applying a dc transport current and measuring the voltage in the standard four-point configuration. In the transport data presented in this work, the magnetic field was mainly normal to the surface of the film ($\mathbf{H} \parallel \mathbf{c}$). The cases where the presented data refer to a field parallel to the film's surface, will be explicitly specified. For both field orientations, the applied current was normal to the magnetic field $\mathbf{J}_{dc} \perp \mathbf{H}_{dc}$, so that the vortex lines experience a non-zero Lorentz force $\mathbf{F}_L \propto \mathbf{J}_{dc} \times \mathbf{H}_{dc}$. In our magnetoresistance measurements we also employed the ZFC initial conditions. Thus, a direct comparison with our magnetic data could be made safely. The temperature control and the application of the dc fields in our transport measurements were achieved in our SQUID magnetometer. We examined the whole temperature-magnetic-field regime accessible by our SQUID ($H_{dc} < 55 \text{ kOe}$, $T > 1.8 \text{ K}$).

EXPERIMENTAL RESULTS AND DISCUSSION FOR SAMPLE NB-1

Thermomagnetic instabilities and the "second magnetization peak"

We start the presentation of our experimental results for sample Nb-1, which in the low-temperature regime

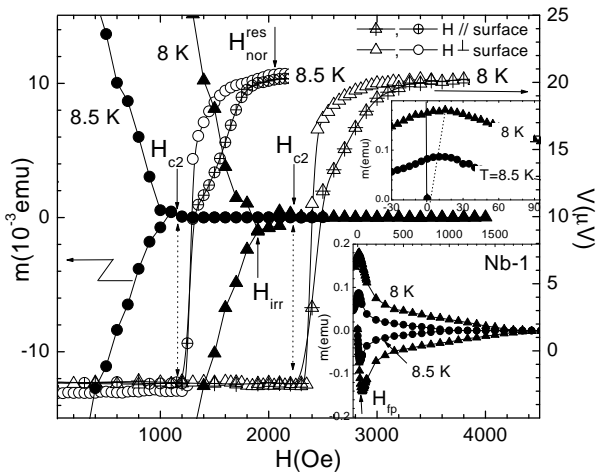


FIG. 1: Isothermal magnetic $m(H)$ and magnetoresistance $V(H)$ measurements for the film Nb-1 (solid and open points respectively) in two representative temperatures $T = 8$ and 8.5 K, focused in the regime of the upper-critical field H_{c2} . The solid and open points without (with) crosses refer to the case where the magnetic field is normal (parallel) to the surface of the film. In both transport data the applied current ($I_{dc} = 1$ mA) was normal to the magnetic field $\mathbf{J}_{dc} \perp \mathbf{H}_{dc}$. The first inset presents the whole loops, so that the first peak H_{fp} may be seen, while the second inset focusses on the descending branch of the loops so that the respective peak may be observed.

exhibits the TMI and the "SMP". Figure 1 presents magnetic measurements in comparison to transport data, in the high-temperature regime, for two representative temperatures $T = 8$ and 8.5 K. In magnetic measurements the applied field is normal to the surface of the film (as in all the magnetic data presented in this work), while in transport data we present both cases where the field is normal (open points) and parallel (points with crosses) to the surface of the film.

First of all, we see that, with high accuracy, the measured voltage becomes non-zero at the magnetically determined upper-critical points H_{c2} (where the magnetic moment vanishes). The simultaneous occurrence of the resistive and the magnetic transitions is expected in conventional low- T_c superconductors [27]. We observe that the comparison of transport data to magnetic measurements is very informative. A lack of such a comparison could mistakenly lead to the interpretation of a melting transition at the points where the sharp drop in the voltage curves is observed. Our results reveal that in low- T_c superconductors, sharp resistance drops are also caused by the conventional transition between the normal and superconducting states. Above the upper-critical points H_{c2} we observe a rounding of the measured voltage curve, which attains the normal state value at a much higher field H_{nor}^{res} . This feature is more evident when the magnetic field is parallel to the surface of the film (symbols

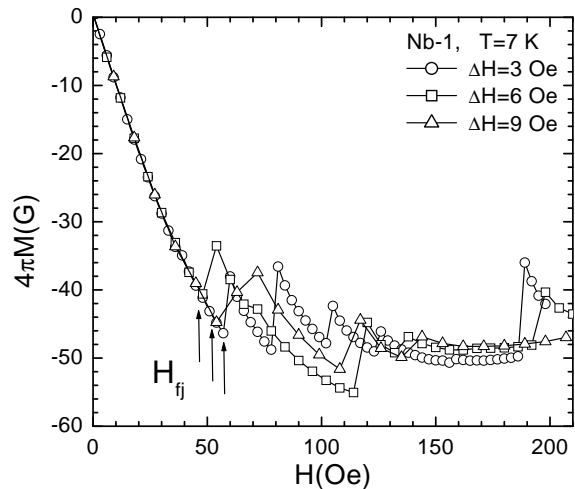


FIG. 2: Isothermal magnetization curves $4\pi M(H)$ for film Nb-1 at $T = 7$ K, for three different sweep rates of the magnetic field with steps $\Delta H = 3, 6$ and 9 Oe. We observe that for higher sweep rate of the magnetic field, flux jumps are more rare. In the resulting magnetization curves demagnetization corrections have been taken into account [30, 31].

with crosses), indicating that it is probably related to surface superconductivity (see below) [27, 28]. In the lower inset we present the whole magnetic loops so that the first peak H_{fp} may be seen. The upper inset focusses in the low-field part of the descending branch so that the respective peak may be easily seen. We observe that the peak of the descending branch is placed in positive field values. In a recent work Shantsev et al. [29] have studied the position of the peak observed in the descending branch in $m(H)$ loops when the magnetic field is normal to a superconducting specimen. They concluded that this peak is placed to positive field values when the sample exhibits a granular structure [29]. In our case TEM data revealed that the Nb-1 film exhibits a slight tendency for columnar growth (see below). Thus, in agreement to Ref. 29 we suggest that the peak of the descending branch is placed to positive field values due to the underlying columnar growth of the Nb-1 film.

In fig. 2 we present magnetization measurements [30, 31] for $T = 7$ K and for different field sweep rates, focused in the low-field regime where the first peak H_{fp} should be expected. In contrast to the smooth curves which are observed at temperatures close to T_c , we see that for $T = 7$ K flux jumps are present. The observed flux jumps are small, of the order of a few Gauss to less than twenty Gauss. More importantly, the flux jumps depend on the sweep rate of the field. As we increase the sweep rate, the flux jumps are rare. At even lower temperatures the magnetic response becomes more anomalous. At $T = 6$ K a broad "noisy" first peak shows up, which at lower temperatures transforms into two separate peaks: a first maximum which occurs in low-field

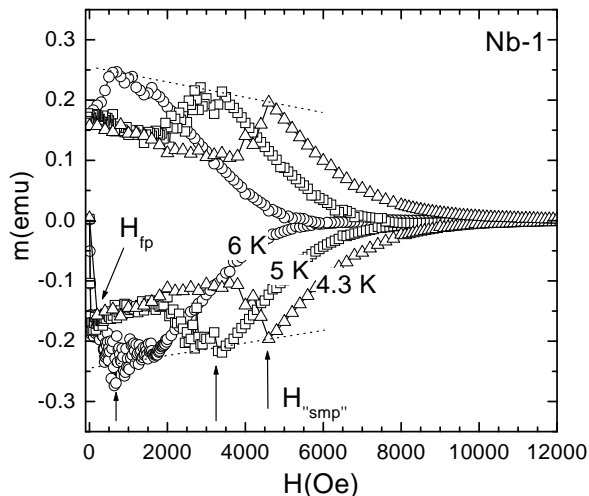


FIG. 3: Isothermal magnetic moment $m(H)$ measurements for Nb-1 sample, in the low-temperature regime at $T = 4.3, 5$ and 6 K. In addition to the first peak H_{fp} , which is placed in the low-field regime, we observe a "SMP" in higher magnetic fields H'_{smp} . The peak value of the "SMP" decreases for lower temperatures (see dot lines which serve as guides to the eye).

values, and a distinct second peak which is placed in high magnetic fields. This behavior may be seen in fig. 3 for three representative temperatures $T = 4.3, 5$ and 6 K. The overall behavior resembles the SMP observed usually in high- T_c superconductors [16, 17, 18, 19, 20]. For this reason we "loosely" refer to these characteristic fields as H'_{smp} . However, there are noticeable differences between the magnetic behaviors observed in Nb-1 and in high- T_c superconductors. Below the "SMP" ($H < H'_{smp}$) the response is "noisy", while above it ($H > H'_{smp}$) we observed smooth magnetic curves. In contrast, in *point disordered* high- T_c superconductors the magnetization curves are smooth, both below and above the SMP. In addition, the peak value of the H'_{smp} slightly decreases as we lower the temperature (see fig. 3). In high- T_c superconductors for lower temperatures the peak value of the SMP strongly increases [16, 17, 20]. Finally, the resulting line $H'_{smp}(T)$ ends on the first peak line $H_{fp}(T)$ at $T_o/T_c \approx 0.78$ in our Nb-1 film (see fig. 7(b) below), while in high- T_c superconductors the respective line $H_{smp}(T)$ ends near the irreversibility/melting line, or extends almost up to the critical temperature.

In a recent theoretical study Mints and Brandt [32] considered the special case where TMI occur in superconducting films when the magnetic field is normal to the film's surface. They derived the following criterion for the first field value H_{fj} where flux jumps occur

$$\frac{H_{fj}(T)\mu_0\dot{H}l}{\kappa(T)q^2j_c(T)} \frac{dj_c(T)}{dT} = 1, \quad (1)$$

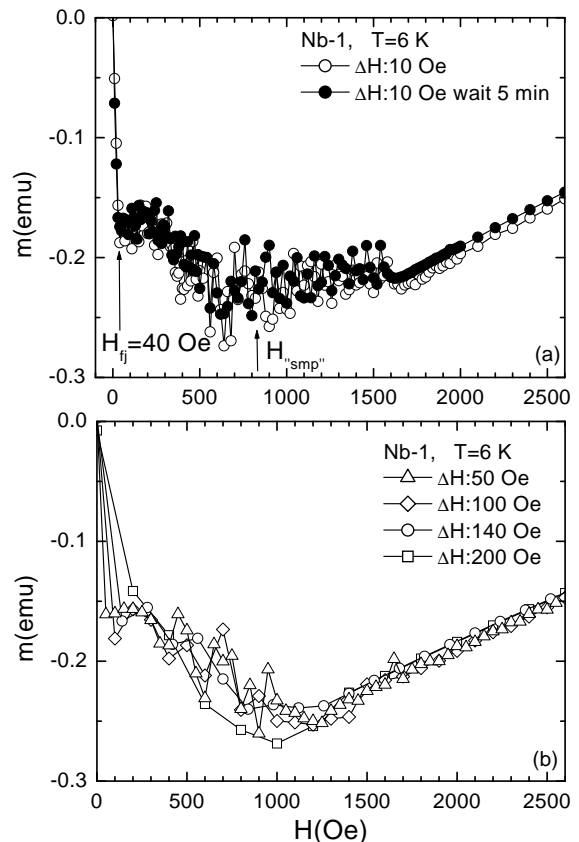


FIG. 4: Isothermal magnetic moment $m(H)$ measurements for film Nb-1 at $T = 6$ K, for different application rates of the magnetic field with steps, $\Delta H = 10$ Oe (upper panel) and $\Delta H = 50, 100, 140$ and 200 Oe (lower panel). When introducing a high enough sweep rate of the magnetic field (lower panel), the measured curves exhibit flux jumps more rarely. For the case where $\Delta H = 10$ Oe (upper panel) we performed exactly the same measurement when introducing a waiting time of 5 min before start measuring (after the application of the new field value). We see that the magnetic behavior is exactly the same as when measuring right after the application of the field.

in where \dot{H} is the sweep rate of the applied field, l is the exponent of the $J - E$ characteristic ($J(E) = J_c(E/E_0)^{1/l}$), $\kappa(T)$ is the thermal conductivity and q is a parameter that accounts for the thermal boundary resistance between the film and the substrate. This model that deals with an experimentally realizable case, predicts that the first flux jump field H_{fj} decreases as the sweep rate \dot{H} of the applied field and the exponent l of the $J - E$ curves increase.

In order to test the theoretical predictions we performed systematic magnetic measurements for various sweep rates of the applied field. In fig. 4 we present such data at temperature $T = 6$ K. We observe that as we increase the sweep rate of the applied field, the flux jumps are rare. This indicates that the flux jumps can

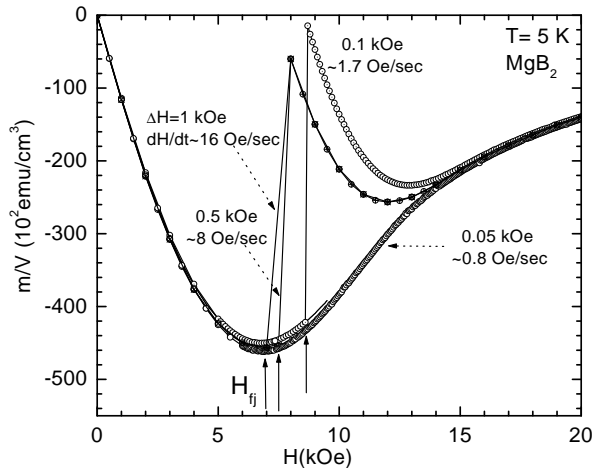


FIG. 5: Isothermal magnetic $m(H)$ measurements in a bulk sample of MgB_2 for $T = 5$ K, and for various steps of the applied field $\Delta H = 1, 0.5, 0.1$ and 0.05 kOe. The first flux jump field H_{fj} is placed to lower values when increasing the sweep rate of the applied field \dot{H} .

not be detected in high electric-field levels (where vortices are probably unpinning) but are present only when we probe the vortex system in very low electric-fields. Furthermore, we studied in detail the dependence of the first flux jump field H_{fj} on the sweep rate of the magnetic field for steps ΔH low enough, so that H_{fj} could be defined accurately. In measurements (not shown here) performed with steps ΔH in the range $2 \text{ Oe} < \Delta H < 15 \text{ Oe}$, we observed that the field H_{fj} remained constant, $H_{fj} = 40 \text{ Oe}$. This is in contrast to theoretical expectations. Our results are in agreement to the experimental studies of Ref. 14. On the other hand, such anomalous flux jumps could be an artifact, caused by the inability of our SQUID to maintain a constant temperature on the whole film. To test this case we performed exactly the same measurement for step $\Delta H = 10 \text{ Oe}$, after having waited for 5 min before measuring. The result is presented in fig. 4(a). We clearly see that the flux jumps are still present.

Very recently it was discovered that the compound MgB_2 is a superconductor with relatively high critical temperature $T_c = 39 \text{ K}$. As a result of the renewed interest, many groups have done reliable studies on TMI in MgB_2 samples, either in thin film or in bulk form, by performing thorough magnetic measurements, or by using more direct techniques such as magneto-optical imaging [33, 34, 35, 36]. The observed behavior in MgB_2 films is very similar to the behavior that we observed in our Nb films. Thus, in a next section we compare our experimental results to recent results obtained in MgB_2 films. On the other hand, currently available theories distinguish the driving mechanisms of TMI when observed in thin films or in bulk samples. In order to directly compare the

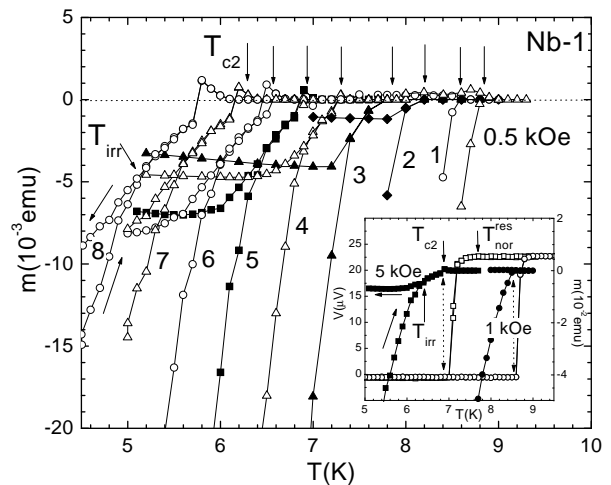


FIG. 6: Isofield magnetic measurements $m(T)$ for Nb-1 under various magnetic fields $H = 0.5 - 8$ kOe. We focus in the regime near the upper-critical points T_{c2} so that the irreversibility points T_{irr} may be seen. The inset presents, comparatively, magnetic and voltage measurements as a function of temperature, at fields $H = 1$ and 5 kOe. We observe the congruence of the magnetic and the resistive transitions (see dot arrow lines). At the irreversibility points T_{irr} the voltage does not show any measurable feature.

two cases, we also present magnetic measurements performed in a bulk sample of MgB_2 superconductor [37]. The preparation process is reported elsewhere [38]. In fig. 5 we observe that by decreasing the sweep rate of the field, the first flux jump field H_{fj} increases. This is in agreement to theoretical expectations for bulk samples [39, 40]. In contrast, in the Nb-1 film the field H_{fj} doesn't exhibit such behavior, as already discussed above. In our bulk MgB_2 sample, TMI are not observed for low sweep rates of the applied field, $\dot{H} < 1 \text{ Oe/sec}$. On the other hand, for $\dot{H} > 1 \text{ Oe/sec}$, flux jumps are observed that are comparable to the measured magnetic moment. Thus, after every flux jump the sample almost enters the normal state. We may then refer to a global thermal runaway as the underlying mechanism of TMI in this bulk sample. In contrast, the flux jumps observed in our Nb-1 film are much smaller than its magnetic moment and don't turn the sample in the normal state. Finally, in our MgB_2 bulk sample, the first flux jump field H_{fj} is placed above the full penetration field, which may be fairly approximated by the first peak field H_{fp} . This is in contrast to theoretical expectations [39, 40]. In the Nb-1 film, we observed that when the first flux jump field H_{fj} exceeds the first peak field H_{fp} , TMI are no longer present (see figs.7 and 9 below). The differences mentioned above indicate that the mechanism of TMI is not only quantitatively, but could be also qualitatively different between bulk and film samples.

Phase diagram of vortex matter for Nb-1.
Comparison with theory

In order to construct the phase diagram of vortex matter for Nb-1 film, we also performed isofield magnetic measurements as a function of temperature. Representative data are shown in fig. 6. We mainly focus near the transition to the normal state, so that the irreversibility points T_{irr} may be easily seen. The inset presents comparative magnetic moment and voltage measurements as a function of temperature. We observe that as we increase the applied field, the regime of magnetic reversibility is enhanced. In addition, the magnetic and the resistive transitions clearly coincide, in agreement to our isothermal measurements as a function of field (see fig. 1). At the irreversibility points T_{irr} the measured voltage curves do not show any distinct feature.

The resulted "phase diagram" for the film Nb-1 is presented in figs. 7(a) and 7(b). Open (solid) triangles, coming from magnetic measurements as a function of field (temperature), denote the irreversibility fields $H_{irr}(T)$ (temperatures $T_{irr}(H)$), while open and solid squares (from magnetic measurements as a function of field and temperature, respectively) refer to the magnetically determined upper-critical fields $H_{c2}(T)$ and temperatures $T_{c2}(H)$. Furthermore, the semi-filled squares refer to the characteristic line $H_{nor}^{res}(T)$ where the resistance takes the normal state value. In the low-field regime, presented in detail in fig. 7(b), the rhombi originate from the "SMP", while the open circles refer to the first peak field $H_{fp}(T)$ (for $T > T_o = 7.2$ K) and to the first flux jump field $H_{fj}(T)$ (for $T < T_o = 7.2$ K).

First of all, we observe that the $H_{irr}(T)$ data exhibit a slight upward curvature, which is reminiscent of the behavior observed in type-II high and low- T_c [4, 5, 6, 17, 19], or even type-I [41] superconductors. As we clearly see, the irreversibility points $T_{irr}(H)$ as determined from isofield magnetic measurements as a function of temperature (solid triangles), do not coincide with the respective points $H_{irr}(T)$ as determined from isothermal magnetic loop measurements (open triangles). This is a consequence of their dynamic origin. The irreversibility points, as determined from such measurements, simply mark the boundary where the vortex system is at a pseudo-equilibrium state for the specific measuring time of every experiment. Thus, the irreversibility points ($H_{irr}(T)$ or $T_{irr}(H)$) should not be attributed to the points where a melting transition of vortex matter takes place, as in the past has been reported for the case of sputtered Nb films [6]. Detailed transport measurements of the $I-V$ characteristics that we performed give additional evidence to this point of view. Representative data are shown in fig. 8 for $T = 8$ K and various magnetic fields in the regime close to the upper-critical field $H_{c2}(8K)$. In the inset we present a detail of the respective part of the phase diagram where the measurements

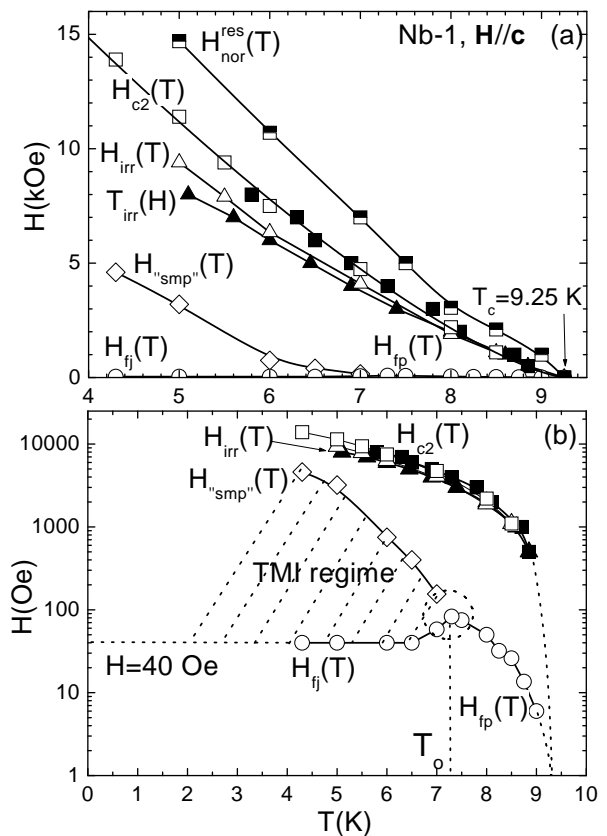


FIG. 7: Resulted phase diagram for the Nb-1 film ($H \parallel c$). Presented are the $H_{fp}(T)$ and $H_{fj}(T)$ lines (low-field open circles), the "SMP" line $H_{smp''}(T)$ (rhombi), the $H_{irr}(T)$ (triangles) and the upper-critical field $H_{c2}(T)$ (squares) lines (where open points come from isothermal $m(H)$ measurements, while solid points come from isofield $m(T)$ measurements). The solid line through the $H_{c2}(T)$ points, is a least squares fitting by using the expression $H_{c2}(T) = H_{c2}(0)(1 - T/T_c)^m$ with $H_{c2}(0) = 31.8 \pm 0.8$ kOe and $m = 1.34 \pm 0.03$. In the upper panel we also included the characteristic field line $H_{nor}^{res}(T)$ where the voltage takes the normal state value. The lower panel reveals the details of the features observed in the low-field regime in semi-logarithmic scale.

have been performed (shaded area). We clearly see that even in the regime above the magnetically determined irreversibility field $H_{irr}(8K)$ the $I-V$ characteristics are non-linear and gradually attain an almost linear behavior as the upper-critical field $H_{c2}(8K)$ is approached. This means that in low- T_c superconductors the irreversibility points can not be ascribed to a true melting transition since a true liquid state should be accompanied by absolutely linear behavior in the $I-V$ curves. Furthermore, even above the upper-critical field a slight nonlinearity is maintained in the $I-V$ curves which is removed only above the characteristic field $H_{nor}^{res}(8K)$ where the voltage attains its normal state value. This fact indicates that the regime $H_{c2}(T) < H < H_{nor}^{res}(T)$ of the phase diagram

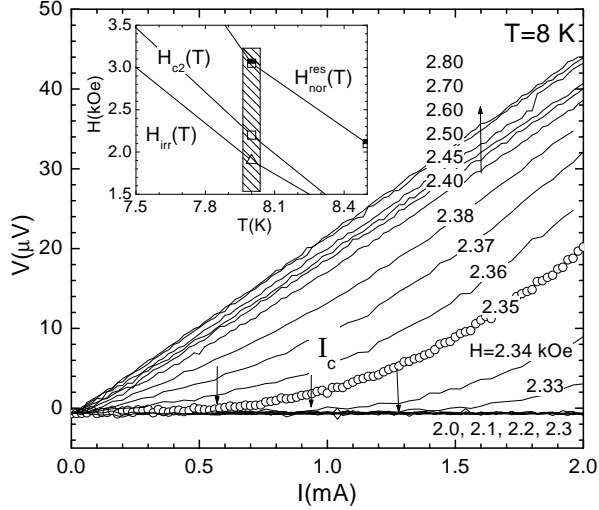


FIG. 8: Detailed measurements of the $I - V$ characteristics at $T = 8$ K and for various magnetic fields $2 \text{ kOe} < H < 2.8$ kOe (main panel) and a detail of the phase diagram where the measurements have been performed (inset). Despite the fact that some of the transport measurements were performed inside the magnetically reversible regime a linear behavior of the $I - V$ curves (expected in a liquid state of flux lines) was not observed. The Ohmic behavior is recovered gradually in the regime $H_{c2}(8\text{K}) < H < H_{\text{nor}}^{\text{res}}(8\text{K})$.

refers to surface superconductivity (see below) [27, 28]. Finally, we note that the present data suggest that the Nb-1 film is quite disordered since even at $H = 2.3$ kOe $\simeq H_{c2}^{\text{mag}}(8\text{K})$ the maximum applied current $I_{\text{dc}} = 2$ mA is not able to depin vortices. By taking into account the dimensions of the specific film we estimate the effective current density which for the case under discussion ($T = 8$ K, $H = 2.3$ kOe) is $J_{\text{dc}} \simeq 0.1 \text{ kA/cm}^2$. Thus, at $T = 8$ K, $H = 2.3$ kOe the critical current density J_c exceeds 0.1 kA/cm^2 .

Let us now return to the discussion of the phase diagram presented in figs.7(a) and 7(b). We see that in contrast to the irreversibility points $H_{\text{irr}}(T)$ the upper-critical points $H_{c2}(T)$ as determined from the two kind of measurements coincide entirely. Interestingly, the line $H_{c2}(T)$ also presents an upward curvature. These data are fitted nicely by the expression $H_{c2}(T) = H_{c2}(0)(1 - T/T_c)^m$, where $H_{c2}(0) = 31.8 \pm 0.8$ kOe and $m = 1.34 \pm 0.03$. Finally, we observe that the resistive transition is accomplished at even higher fields $H_{\text{nor}}^{\text{res}}(T)$. The $H_{\text{nor}}^{\text{res}}(T)$ line may mark the onset of surface superconductivity [27, 28], as usually observed in other low- T_c superconductors [42, 43]. Transport data and the concept of surface superconductivity will be presented and discussed in detail for the Nb-2 film (see below).

One of the main results of the present paper, regarding the subject of TMI, is shown in the low-field regime as presented in detail in fig. 7(b). We see that the

$H_{\text{fp}}(T)$, $H_{\text{fj}}(T)$ and $H_{\text{smp}}''(T)$ lines connect at a characteristic point $(H, T) \approx (80 \text{ Oe}, 7.2 \text{ K})$. The $H_{\text{smp}}''(T)$ line is placed in high fields, while the $H_{\text{fj}}(T)$ line gradually moves in lower fields and below $T \approx 6.4 \text{ K}$ takes the constant value $H_{\text{fj}}(T < 6.4\text{K}) = 40 \text{ Oe}$. This experimental fact, of a temperature independent $H_{\text{fj}}(T)$ line, is in contrast to theoretical predictions that treat the $H_{\text{fj}}(T)$ line as a simple boundary above which TMI occur [32, 39, 40, 44]. Indeed, within the adiabatic approach and the Bean model [39, 40, 44], for the case of bulk samples, the first flux jump field H_{fj} exhibits a temperature variation due to its dependence on the critical current $j_c(T)$ and on the specific heat $C(T)$, as

$$H_{\text{fj}}(T) = \sqrt{\pi^3 C(T) \frac{j_c(T)}{\left| \frac{dj_c(T)}{dT} \right|}}. \quad (2)$$

We may assume that in Nb, the specific heat in the superconducting state is fairly described by $C(T) \approx C_o T^3$, and that the non-linear temperature dependence $j_c(T) = j_o[1 - (T/T_c)^n]^m$ holds for the critical current, in the most general case. The result for the first flux jump field is

$$H_{\text{fj}}(T) = H_o T^2 \sqrt{\left(\frac{T_c}{T}\right)^n - 1}, \quad (3)$$

where $H_o = (\pi^3 C_o / nm)^{1/2}$.

For the case of thin films, by rewriting Eq. 1, the first flux jump field is given by [32]

$$H_{\text{fj}}(T) = \frac{1}{\mu_0 \dot{H} l} \frac{\kappa(T) q^2 j_c(T)}{\left| \frac{dj_c(T)}{dT} \right|}. \quad (4)$$

For Nb the thermal conductivity is described by the relation $\kappa(T) \approx \kappa_o T^\kappa$. In the superconducting state ($3 \text{ K} < T < T_{c2}(H)$) the exponent κ takes the values $1 < \kappa < 3$ [45]. By assuming the general relation $j_c(T) = j_o[1 - (T/T_c)^n]^m$ for the critical current, we arrive to the following equation

$$H_{\text{fj}}(T) = H_1 T^{\kappa+1} \left[\left(\frac{T_c}{T}\right)^n - 1 \right], \quad (5)$$

where $H_1 = (\kappa_o q^2 / \mu_0 \dot{H} l n m)$.

A condition needed for flux jumps to occur is that the first flux jump field $H_{\text{fj}}(T)$ is placed below the full penetration field [39, 40], which may be experimentally approximated by the first peak field $H_{\text{fp}}(T)$. So, when $H_{\text{fj}}(T) < H_{\text{fp}}(T)$ flux jumps are expected while above a characteristic temperature T_o , where $H_{\text{fj}}(T > T_o) > H_{\text{fp}}(T > T_o)$, flux jumps should not be observed. For the case of a strip, the full penetration field is given by [46]

$$H_{\text{fp}}(T) = \frac{d}{\pi} [1 + \ln(\frac{w}{d})] j_c(T), \quad (6)$$

where w and d are the width and the thickness of the film respectively, and $j_c(T) = j_o[1 - (T/T_c)^n]^m$ in the most

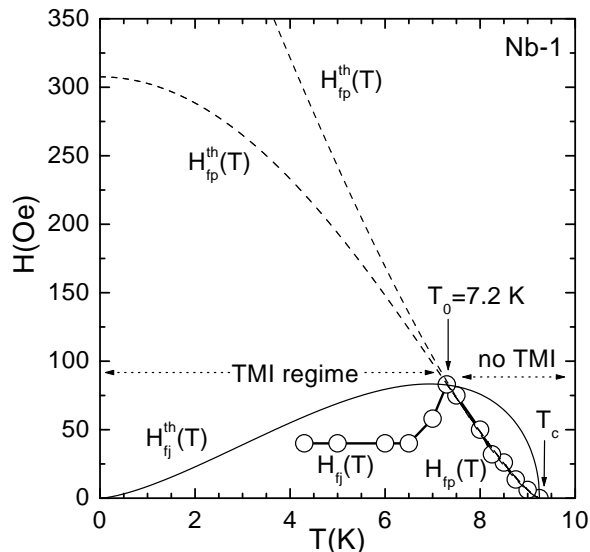


FIG. 9: Experimental data (circles) and theoretical fitting curves by using Eq. 7 (dot lines) for the first peak field $H_{fp}(T)$ for $T > T_o$. In the temperature regime $T < T_o$ the data refer to the first flux jump field $H_{fj}(T)$, while the solid curve reproduces the theoretical expression of Eq. 3 with the parameters $H_o = 3$ and $n = 1$. We observe the inability of the theoretical curve (solid line) to describe the experimental data (see text for more details).

general case. So, the first peak field exhibits a behavior of the form

$$H_{fp}(T) = H_2 \left[1 - \left(\frac{T}{T_c} \right)^n \right]^m, \quad (7)$$

with $H_2 = (d/\pi)[1 + \ln(w/d)]j_o$.

In fig. 9 we present the comparison of our experimental data to the outlined theoretical suggestions. We clearly see that in the temperature range $T > T_o = 7.2$ K, where the line $H_{fj}(T)$ tends to overcome the first peak line $H_{fp}(T)$, TMI are no longer observed. In this temperature regime ($T > T_o = 7.2$ K), the first peak field $H_{fp}(T)$ is experimentally well defined, and is described nicely by the theoretical expression of Eq. 7. The dotted curve, placed at high fields, refers to the fitting parameters $n = 1$, $m = 1.34$ and $H_2 = 686 \pm 11$ Oe, while the dotted one which is placed in lower fields, is described by $n = 2$, $m = 1.34$ and $H_2 = 308 \pm 5$ Oe. The different exponents $n = 1$ and 2 refer to the most common cases discussed in the literature, where the critical current exhibits a linear and a quadratic dependence on T/T_c . We must underline that in both cases the critical temperature was treated as a constant, equal to the real $T_c = 9.25$ K, and the exponent $m = 1.34$ has the same value as in the case of the fitting procedure for the upper-critical field $H_{c2}(T)$ (see fig. 7(a)). In contrast, regarding $H_{fj}(T)$ in the regime $T < T_o = 7.2$ K the experimental data are not described by any theoretical curve. The solid line

reproduces the theoretical curve of Eq. 3 for the parameters $H_o = 3$ and $n = 1$. This expression holds for the case of bulk samples. The relation 5, that refers to thin films, also fails to reproduce our experimental data, regardless of the choice for the exponents κ and n .

As we noticed above, the main discrepancy between current theoretical suggestions and our experimental results, is the low temperature behavior of the first flux jump line $H_{fj}(T)$. Our data clearly show that for $T < 6.4$ K the $H_{fj}(T)$ line is actually constant, $H_{fj}(T < 6.4K) = 40$ Oe. Let us assume that Eq. 4 (referring to a thin film sample), or even Eq. 2 (referring to bulk samples) should be used to describe the low-temperature part of our $H_{fj}(T)$ line. The left side of these equations should then be treated as a constant. By solving these simple differential equations, we easily see that a constant first flux jump line $H_{fj}(T)$ requires an exponential temperature decrease of the critical current $j_c(T) = C_1 \exp(-C_2 T^p)$ ($p > 0$). This is at odds to well known theoretical results or experimental findings that deal with the pinning mechanism of vortices and the temperature variation of the critical current $j_c(T)$ in low- T_c superconductors. More theoretical work is needed in order to resolve this discrepancy.

Comparison with magneto-optical studies

Let us now compare our results to recent magneto-optical studies. Such studies performed in Nb films of similar thickness (5000 Å), dimensions (3×8 mm²) and quality ($T_c = 9.1$ K) as our films, revealed that below the reduced temperature $T/T_c \approx 0.65$, the penetration of magnetic flux takes place in the form of dendrites [47]. In our case the "SMP" line $H'_{smp}(T)$ ends at $T_o \approx 7.2$ K, which in reduced temperature units is $T_o/T_c \approx 0.78$. Duran et al. showed that once a dendrite is formed, it remains "frozen in place" until the magnetic field is changed sufficiently, so that a new structure to appear [47]. In our Nb films we observed that when having waited for 5 min before measuring, the structure of the resulted loops remained exactly the same (with slightly lower values due to the relaxation of the magnetization, see fig. 4(a)). This probably indicates a "stationary" character of the vortex penetration process. This result may have a common origin with the dendrites that were observed in Ref. 47 to remain "frozen in place".

For the case of thin films of the recently discovered superconductor MgB₂ it was proved that such dendritic instabilities, as the ones observed by Duran et al. in Nb, [47] are directly related to the flux jumps occurring in magnetization measurements [33, 34, 35, 36]. This has also been confirmed recently in Nb₃Sn films [48]. On the other hand, the magnetic studies of Refs. 33, 34, 35, 36 and 48 didn't exhibit a "SMP". Despite that, the overall similarity of their observations on TMI with our results,

prompts us to assume that even for the case of Nb films the flux jumps, and consequently the formation of the "SMP", are probably related to dendrites of vortices. Recent numerical simulations on magnetic flux penetration in type-II superconductors also advocate to this point of view [49]. It would be interesting if magneto-optical studies could reveal new information about the possible relation of dendritic structures and the "SMP" observed in our Nb-1 film.

EXPERIMENTAL RESULTS AND DISCUSSION FOR SAMPLE NB-2

Magneto-resistance measurements and the peak effect

The situation is different for the Nb-2 film, which is thinner (1600 Å) and is produced without annealing during the deposition. Figure 10 presents two sets of magneto-resistance measurements, performed at different directions of the external magnetic field. At the first set (dotted curves) the dc field was normal, while at the second set (solid curves) was parallel to the surface of the film. In both sets of data we observed a sharp decrease of the voltage at the end points T_{ep} , which are denoted by the inclined arrows. Above T_{ep} , the voltage curves gradually take the normal state value at the characteristic points T_{nor}^{res} . Furthermore, we see that the sharp drop of the voltage at points T_{ep} becomes more evident when high magnetic fields are applied. Interestingly, the situation is analogous to the results observed by magnetotransport measurements for the case of the cubic (K,Ba)BiO₃ superconductor in Ref. 50. In our case, as in that study, the voltage takes about 95% of its normal state value at T_{ep} , and after increases up to 100% at T_{nor}^{res} .

Careful measurements, performed in the whole temperature regime of the mixed state, in the Nb-2 film, revealed that for $T < T_{ep}$ the signal is not really zero (as happened in film Nb-1) but possesses structure. In fig. 11 we present, in a semi-logarithmic plot, representative measurements for the case where the magnetic field is normal to the film's surface, ($\mathbf{H} \parallel \mathbf{c}$). We observe that, in addition to T_{ep} , the measured voltage curves exhibit two more characteristic points. First, a local peak at T_{onset} , and second a dip at T_{peak} . This is the well-known PE in the critical current J_c (the minimum in the measured voltage corresponds to a maximum/peak in the critical current J_c), which was observed in high- T_c compounds [4, 17, 18, 51], in superconductors of intermediate- T_c as pristine and Carbon-doped MgB₂ [42, 52, 53], in Nb [9, 10, 54, 55, 56] and other low- T_c [4, 57, 58, 59] disordered superconductors. The comparison to our magnetic measurements (not shown here) revealed that the PE almost coincides with the upper-critical fields (see fig. 13 below). As we move in the high-temperature regime the

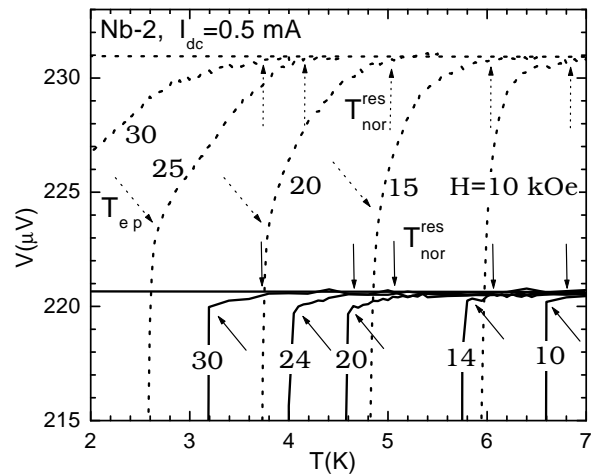


FIG. 10: Measured voltage as a function of temperature for film Nb-2, under various magnetic fields when normal (dot curves) and when parallel (solid curves) to the surface of the film. In both cases the applied current ($I_{dc} = 0.5$ mA) was normal to the magnetic field $\mathbf{J}_{dc} \perp \mathbf{H}_{dc}$. Inclined arrows denote the end points T_{ep} of the voltage drop, while vertical arrows refer to the points T_{nor}^{res} where the voltage takes the normal state value.

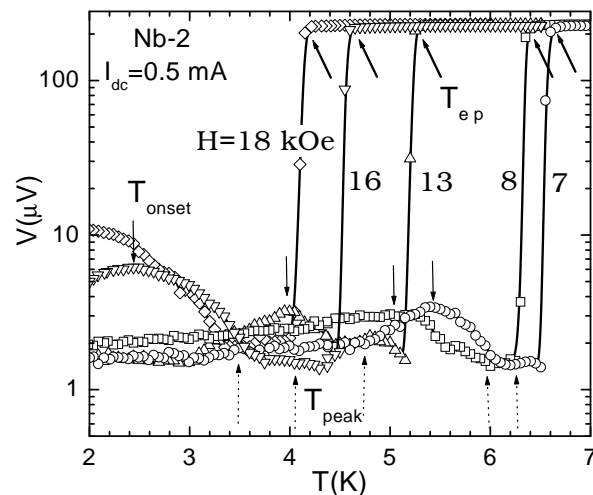


FIG. 11: Semi-logarithmic plot of the measured voltage as a function of the temperature for film Nb-2, under a dc transport current $I_{dc} = 0.5$ mA, for various dc magnetic fields $H_{dc} = 7, 8, 13, 16$ and 18 kOe ($\mathbf{H} \parallel \mathbf{c}$). We observe three characteristic points: (a) T_{onset} where a peak is formed, (b) T_{peak} where the local minimum corresponds to a peak in the critical current and (c) T_{ep} where a sharp increase occurs.

PE is reduced.

A question which remains open is the nature of the PE and of the residual resistive transition in the temperature regime $T_{peak} < T < T_{nor}^{res}$. To investigate the underlying physical processes in detail, we performed measurements for increasing and decreasing the temperature. In

fig. 12(a) we present the results for a constant current, in various dc fields. We observed that in the temperature interval $T_{\text{peak}} < T < T_{e,p}$ the response is hysteretic. The hysteresis is very narrow, $\Delta T < 20$ mK, and is suppressed in the high and low-field regimes, presenting a maximum for intermediate values of the applied magnetic-field. The influence of the transport current on the hysteretic response was also investigated for currents $0.02 \text{ mA} < I_{\text{dc}} < 5 \text{ mA}$. Representative results, for the case where $H_{\text{dc}} = 25 \text{ kOe}$ are summarized in fig. 12(b). For very small transport currents the hysteresis is totally suppressed, as this is evident for the case where $I_{\text{dc}} = 0.05 \text{ mA}$. When the applied current is of intermediate values, hysteretic behavior is clearly detected, as we present for the case where $I_{\text{dc}} = 0.5 \text{ mA}$. For even higher currents the hysteresis is reduced, as this is evident when $I_{\text{dc}} = 1 \text{ mA}$. At the end, for $I_{\text{dc}} > 5 \text{ mA}$ the hysteresis was totally suppressed (curves not shown). We carefully checked the reproducibility of our results. Temperature steps were limited to 10 mK in most of our measurements. In order to ensure thermal homogeneity in the whole film, the temperature sweep was very slow, approximately 6 mK/min. To improve the signal-to-noise ratio, at every temperature we collected data for almost one minute. The observed hysteretic behavior could not be caused by a limited temperature resolution or stabilization inability of our SQUID. Successive measurements, performed under the same experimental conditions, revealed that the resulting curves $V(T)$ coincided within ± 2 mK. In the inset we present the influence of the applied current on the position of the peak as defined from the derivative $dV(T)/dT$. When small currents are applied, the position of the derivative's peak is almost constant but above a threshold value ($I_{\text{dc}} \approx 1 \text{ mA}$) it becomes strongly current dependent. These experimental results for the Nb-2 film are discussed below, where the phase diagram of vortex matter is introduced.

Phase diagram of vortex matter for Nb-2. Comparison with theory and other experimental works

Our experimental results for the configuration where the field is normal to the surface of the film are plotted in fig. 13. In the presented characteristic lines, the upper index *res (mag)* refers to data obtained by resistance (magnetic) measurements. First of all, we see that the onset line $H_{\text{onset}}^{\text{res}}(T)$ saturates in the low temperature regime, and exhibits a monotonic decrease toward T_c . The $H_{\text{peak}}^{\text{res}}(T)$, $H_{e,p}^{\text{res}}(T)$ and $H_{c2}^{\text{mag}}(T)$ lines maintain a linear temperature dependence in the whole region investigated here. In the regime close to T_c , the onset and the PE lines are strongly suppressed. Maybe this is not the actual behavior of vortex matter but it is caused by the limited resolution of our voltmeter. Despite that, the

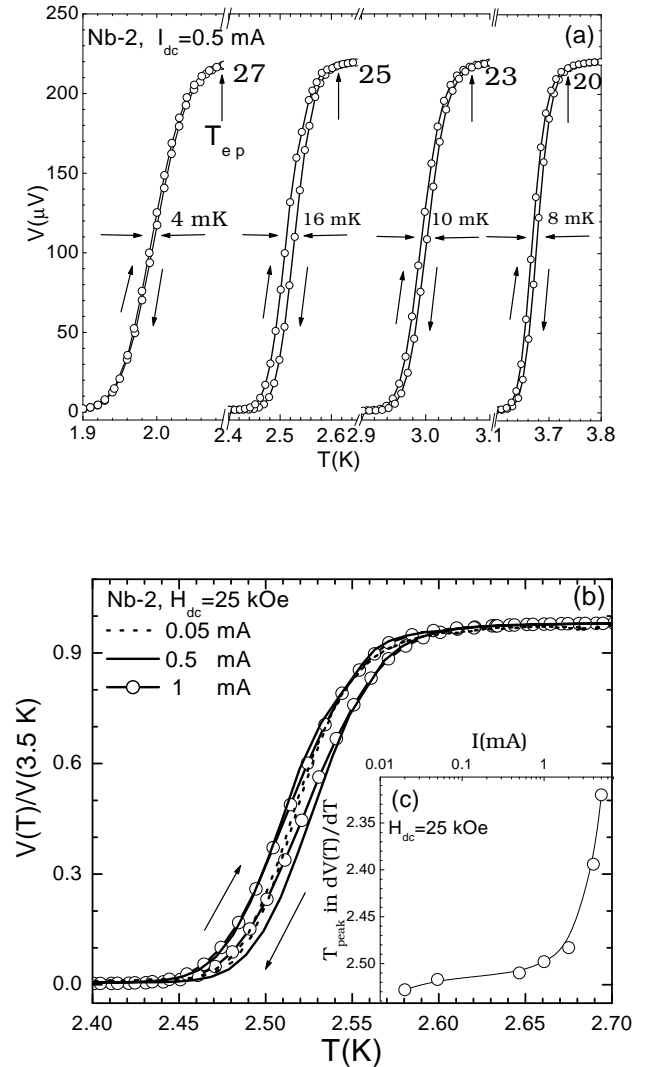


FIG. 12: Measured voltage while increasing and decreasing the temperature for Nb-2 (a) under a dc transport current $I_{\text{dc}} = 0.5 \text{ mA}$, for various dc magnetic-fields $H_{\text{dc}} = 20, 23, 25$ and 27 kOe and (b) under a dc magnetic-field $H_{\text{dc}} = 25 \text{ kOe}$ for various dc transport currents $I_{\text{dc}} = 0.05, 0.5$ and 1 mA (the curve corresponding to $I_{\text{dc}} = 1 \text{ mA}$ is shifted for clarity). In the inset (c) we present the variation of the peak in the derivative $dV(T)/dT$ as a function of the applied dc current. In all cases $\mathbf{H} \parallel \mathbf{c}$.

same behavior has been observed in other low- T_c superconductors [4, 8, 57, 59].

The overall behavior presented in fig. 13 is also qualitatively similar to the phase diagrams of vortex matter observed in disordered high- T_c superconductors, where close to the critical temperature, the SMP and/or PE lines are placed very close to the irreversibility line [4, 17, 18, 19, 60, 61, 62]. A quantitative comparison to recently proposed theoretical models could give further information for the underlying mechanisms that motivate the observed similarity.

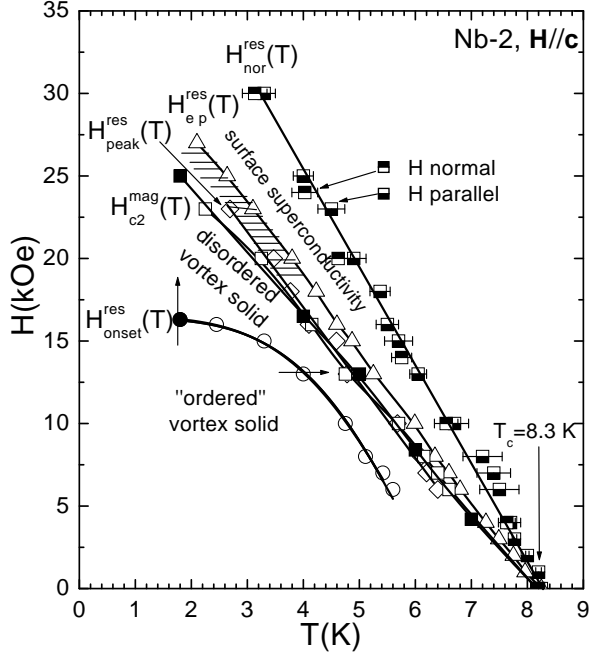


FIG. 13: Phase diagram of vortex matter for the Nb-2 film ($\mathbf{H} \parallel \mathbf{c}$). Presented are the peak's onset $H_{\text{onset}}^{\text{res}}(T)$ (open and solid circles coming from $V(T)$ and $V(H)$ measurements respectively), the peak $H_{\text{peak}}^{\text{res}}(T)$ (rhombi), the end points of the peak $H_{e_p}^{\text{res}}(T)$ (triangles) and the upper-critical field $H_{c2}^{\text{mag}}(T)$ (solid and open squares coming from $m(T)$ and $m(H)$ magnetic measurements respectively), for the case where the magnetic field is normal to the film's surface. Also presented are the field lines $H_{\text{nor}}^{\text{res}}$ (semi-filled squares), at where the voltage takes the normal state value, for both field configurations. The shaded area indicates the regime where hysteretic behavior has been observed in our $V(T)$ curves.

Let us start our discussion with the characteristic line $H_{\text{onset}}^{\text{res}}(T)$ where the onset of the PE occurs. As we see in Fig. 12 these data are placed well inside the mixed state of the superconductor. Recently, it was proposed that an order-disorder transition between two vortex solid states occurs in point disordered superconductors [62, 63, 64]. Experimental studies confirmed the order-disorder transition occurring at (or in close proximity to) the onset of the SMP for disordered high- T_c [18, 62, 65, 66, 67] and at the onset of the PE for the case of low- T_c [58] superconductors. In the "cage model" of Refs. 63 and 64 a pinning parameter γ_p was introduced that characterizes the static disorder. Depending on the particular pinning mechanism the temperature variation of the pinning parameter is: $\gamma_p \sim \lambda^{-4}$ for δT_c pinning (variations in the local transition temperature of the superconductor is the origin of pinning) and $\gamma_p \sim (\xi\lambda)^{-4}$ for δl pinning (variation of the electron mean free path act as pinning centers) [1]. The transition field is estimated by equating the pinning energy to the elastic energy of a vortex. The final expression depends on the relation between three characteristic

lengths of the model: $L_o \approx 2\varepsilon a_o$ which is the length of the "cage" along the c -axis, $L_c = (\varepsilon^4 \varepsilon_o^2 \xi^2 / \gamma_p)^{1/3}$ which is the related pinning length of the vortex and finally d which is the interlayer distance [64]. In these expressions ε is the anisotropy parameter ($\varepsilon = 1$ in our case), a_o is the mean distance of vortices and ε_o is the vortex line energy. By comparing the characteristic length scales we distinguish three cases for the pinning energy: (i) If $d < L_o < L_c$ the pinning energy in the cage is $E_p \approx (\gamma_p \xi^2 L_o)^{1/2} \approx (2\gamma_p \varepsilon a_o \xi^2)^{1/2}$. (ii) When $d < L_c < L_o$ the pinning energy becomes $E_p = E_{\text{dp}}(L_o/L_c)^{(2\zeta-1)}$ with $2\zeta - 1 \approx 1/5$, where $E_{\text{dp}} = (\gamma_p \varepsilon^2 \varepsilon_o \xi^4)^{1/3}$ is the depinning energy of a single vortex line. (iii) Finally, when $L_c < d < L_o$ we have 2D pinning and E_p becomes, $E_p \approx U_p(L_o/d)^{1/5}$, where $U_p \approx \pi \sqrt{\gamma_p \xi^2 / d}$. The vortex lattice to vortex glass transition field is estimated by equating the pinning energy, E_p to the elastic energy, $E_e = \varepsilon \varepsilon_o c_L^2 a_o$ of a vortex. For each of the three cases mentioned above the transition field becomes: (i) when $d < L_o < L_c$ we have $H_{\text{on}}(T) \sim \varepsilon^2 [1 - (T/T_c)^p]^2$ for δT_c pinning, while $H_{\text{on}}(T) \sim \varepsilon^2 [1 - (T/T_c)^p]^{-2}$ for δl pinning, (ii) when $d < L_c < L_o$, $H_{\text{on}}(T) \sim \varepsilon [1 - (T/T_c)^p]^{3/2}$ for δT_c pinning, while $H_{\text{on}}(T) \sim \varepsilon [1 - (T/T_c)^p]^{-1/2}$ for δl pinning. Finally, in case (iii) where $L_c < d < L_o$ (2D pinning regime), $H_{\text{on}}(T) \sim \varepsilon^2 [1 - (T/T_c)^p]^{5/4}$ for δT_c pinning, and $H_{\text{on}}(T) \sim \varepsilon^2 [1 - (T/T_c)^p]^{-5/4}$ for δl pinning (for more details see Refs. 62, 63, 64). For isotropic Nb is reasonable to assume that the conditions $L_o > d$ and $L_c > d$ always hold. We thus fitted the onset points by the proposed expression $H_{\text{on}}(T) = H_o(1 - (T/T_o)^p)^n$, which holds for ΔT_c pinning mechanism. A least squares criterion yielded $H_o = 16.5$ kOe, $T_o = 7$ K if we assume the exponents $p = 4$ and $n = 2$ (case (i)), and $H_o = 16.4$ kOe, $T_o = 6.6$ K if we choose $p = 4$ and $n = 3/2$ (case (ii)) [64]. These fitting curves are denoted in Fig. 12 by two solid lines that coincide in the entire temperature regime. We observe that the equation proposed by the theory describes accurately our experimental results.

The next characteristic line of the phase diagram is the upper-critical field $H_{c2}^{\text{mag}}(T)$, which as we know defines the points where the bulk of the superconductor enters the normal state as we increase the temperature. As we observe, the $H_{c2}^{\text{mag}}(T)$ line coincides entirely with the PE line $H_{\text{peak}}^{\text{res}}(T)$. This has been observed not only in Nb [54, 55, 56], but also in MgB₂ [42] superconductor.

Let us now discuss, in more detail, the possible origin of the $H_{e_p}^{\text{res}}(T)$ and the $H_{\text{nor}}^{\text{res}}(T)$ lines. A brief comparison to other low or even high- T_c superconductors is also made. The main reasons invoked to interpret the irreversible magnetic behavior of isotropic superconductors is the interplay of thermal fluctuations and static disorder on vortex lines. In pure samples, thermal fluctuations transforms the vortex lattice into a liquid of flux lines through a first order transition. This has been observed in the almost isotropic YBa₂Cu₃O_{7- δ} [51, 68, 69]. On the other hand, in disordered samples, it is the static disorder

that transforms the vortex lattice into an amorphous vortex solid. This behavior has been observed in the high- T_c compounds $\text{HgBa}_2\text{CuO}_{4+\delta}$ [18] and $\text{YBa}_2\text{Cu}_3\text{O}_{7-\delta}$ [19] and in the low- T_c superconductors 2H-NbSe_2 [58, 59], CeRu_2 [59] and $\text{X}_3\text{Rh}_4\text{Sn}_{13}$ [4, 57] ($\text{X}=\text{Ca}, \text{Yb}$). In our case, we observed a sharp drop ($\Delta T \approx 100$ mK) at the end points of the PE which is also hysteretic. The observed hysteresis is very narrow ($\Delta T < 20$ mK) and is restricted exclusively in the regime $H_{\text{peak}}^{\text{res}} < H < H_{\text{ep}}^{\text{res}}$ (see shaded area in fig. 13). These experimental facts resemble the melting transition of vortex matter. On the other hand, the sharp hysteretic drop, in the measured voltage, occurs in the regime *above the magnetically determined upper-critical field line* $H_{c_2}^{\text{mag}}(T)$, placing beyond dispute that this effect doesn't refer to a property of vortex matter. But one could object that our SQUID magnetometer may underestimate the true upper-critical fields in our thin Nb-2 film (thickness=1600 Å), due to its limited resolution. Even if this is true, there is a number of additional arguments against a true solid-liquid phase transition. First, the observed hysteresis faints when very low transport currents are employed. This is not compatible to what is expected for a transition of equilibrium origin, as was observed in YBCO [51, 68, 69]. Second, the decrease in the measured voltage at the points T_{ep} is unconventionally high, when compared to the resistive drop at the melting transition in YBCO [51, 68]. In addition, for the case of the melting transition of vortex matter in YBCO, the temperature sweeping down branch was placed above the sweeping up one [51, 68, 69], while in our case we observed the opposite behavior. These facts prevent us from attributing the observed sharp features to the melting transition, in contrast to previous studies in isotropic Nb films [6] or even in MgB_2 single crystals [70].

It could be proposed, that the residual part of the resistive transition in the regime $H_{c_2}^{\text{mag}}(T) < H < H_{\text{nor}}^{\text{res}}(T)$ (see fig. 13), is motivated by the mechanism of surface superconductivity. Then the sharp hysteretic response, restricted in the regime $H_{\text{peak}}^{\text{res}}(T) < H < H_{\text{ep}}^{\text{res}}(T)$ (see shaded area in fig. 13), refer to the phase transition at the bulk upper-critical points, or is also motivated by surface superconductivity. Below, let us briefly present the basic aspects of surface superconductivity, so that a comparison with our experimental results could be made. When physical boundary conditions are taken into account for a magnetic field applied parallel to the main surface of a superconductor, a new nucleation field $H_{c_3}(T)$ exists, at where surface superconductivity develops while lowering the temperature [27, 28]. This characteristic field is placed above the true upper-critical field $H_{c_2}(T)$, and is related to it through $H_{c_3}(T) = 1.695H_{c_2}(T)$. For an isotropic superconductor as Nb, the upper-critical field $H_{c_2}(T)$ should be independent of the orientation of the applied field. Thus, we should expect that, similarly, the surface nucleation field $H_{c_3}(T)$ should occur at the same

points $1.695H_{c_2}(T)$, regardless of the orientation of the magnetic field. As is evident in fig. 13 (see also fig. 10), the voltage takes the normal state value at almost the same points $H_{\text{nor}}^{\text{res}}$ in both field configurations. This could be an additional indication that, in both cases, the experimental lines $H_{\text{nor}}^{\text{res}}(T)$ indeed mark the surface superconductivity effect. At zero temperature, the ratio of the surface superconductivity field $H_{\text{nor}}^{\text{res}}(0)$ to the upper-critical field $H_{c_2}^{\text{mag}}(0)$ is $H_{\text{nor}}^{\text{res}}(0)/H_{c_2}^{\text{mag}}(0) \approx 1.45$. This is a reasonable value if we keep in mind that the ratio $H_{\text{nor}}^{\text{res}}(0)/H_{c_2}^{\text{mag}}(0)$ depends on the combination of two structural parameters that may vary from sample to sample: first, the quality of the bulk (reflected in $H_{c_2}^{\text{mag}}(0)$) and second, the quality of the surface (reflected in $H_{\text{nor}}^{\text{res}}(0)$). On the other hand, the original theoretical treatment suggests that the surface nucleation field $H_{c_3}(T)$ should not be observed when the magnetic field is normal to the main surface of the film. In our case, we observed the same qualitative behavior in both field configurations. In the past, Drulis et al. [5] did not observe surface superconductivity in Nb foils for the case where the applied field was normal to the surface of their samples, but only for the parallel field configuration. We note that in Ref. 5 only the regime of relatively low fields ($H < 5$ kOe) was studied. Our results extend to much higher fields ($H \leq 30$ kOe). As is evident in figs. 10 and 13 the effect under discussion is more pronounced in the high field regime, where the lines $H_{\text{ep}}^{\text{res}}(T)$ and $H_{\text{nor}}^{\text{res}}(T)$ diverge substantially. As a consequence, we were able to detect surface superconductivity even for the normal field configuration. Probably, the same behavior would have been observed in Ref. 5, had the measurements been performed in higher applied fields. Therefore, we believe that our results actually extend the currently available experimental data, regarding the surface superconductivity in Nb. The same behavior has been also observed, for the normal field configuration, in the MgB_2 superconductor [42]. This discrepancy between theory and experiment remains to be resolved.

Consequently, regarding the phase diagram of vortex matter for the Nb-2 film, we believe that in the low-temperature-magnetic-field regime a vortex quasi-lattice exists. Through the onset points $H_{\text{onset}}^{\text{res}}(T)$ of the PE, a gradual disordering of the vortex solid takes place as we approach the $H_{c_2}^{\text{mag}}(T)$. This is actually the softening effect of the vortex lattice, as has been proposed by Larkin and Ovchinnikov many years ago [71]. At the end, above the line $H_{c_2}^{\text{mag}}(T)$ the effect of surface superconductivity is observed up to $H_{\text{nor}}^{\text{res}}(T)$.

**CRYSTALLOGRAPHIC DATA AND
COMPARATIVE DISCUSSION FOR THE Nb-1
AND Nb-2 FILMS**

In this last part of the present article we discuss crystallographic results and we make a comparative discussion for the two Nb films, in order to outline the possible mechanism that motivate the observed similarities and/or differences. The resistivity takes almost the same value $\varrho_n \approx 5 - 10 \mu\Omega\text{cm}$ for both Nb films. In addition, the zero temperature values of the coherence length $\xi(0) \approx 100 \text{ \AA}$, the penetration depth $\lambda(0) \approx 900 \text{ \AA}$, and consequently the Ginzburg-Landau parameter $\kappa(0) \approx 9$, are almost the same for the two Nb films [72]. These values are in fair agreement to the ones reported in the past in disordered Nb samples [5, 6, 8, 14]. Interestingly, despite their almost identical values of $\xi(0)$, $\lambda(0)$ and $\kappa(0)$, the two films exhibit a completely different behavior in the mixed state of their vortex phase diagrams. The film Nb-1 (annealed during the deposition) presents the "SMP" and TMI in a great part of its phase diagram, while the film Nb-2 (not annealed during the deposition) exhibits a comparatively smooth PE, confined in the regime of the upper-critical field $H_{c2}(T)$.

We believe that the different behavior of vortex matter, in the two kinds of films, is caused by the different preparation conditions. Our combined x-ray diffraction (XRD) and transmission electron microscopy (TEM) data revealed that by annealing the films during deposition, a larger mean size of the grains is produced, which in this case is 930 \AA for Nb-1 (annealed) and 420 \AA for Nb-2 (not annealed). Furthermore, the grains of the annealed film are oriented, in some degree, with [110] direction perpendicular to the film's surface and exhibit a tendency for columnar growth, while the film produced without annealing doesn't show such a tendency. These crystallographic data may give worthy information for the interpretation of the mixed-state superconducting properties of the two different films. It seems that in the mixed state of film Nb-1 the dynamic behavior of vortices is governed by a correlated type of disorder since its columnar growth could be considered as extended disorder along the boundaries of the columns. This suggestion favorably agrees with the results of Shantsev et al. [29]. In that work [29] it was proved that a granular structure of a superconducting specimen results in a peak in the descending branch of the $m(H)$ loop which is positioned in positive field values. This behavior is observed in our Nb-1 film (see upper inset of fig.1) and could be related to its tendency for columnar growth. On the other hand in film Nb-2 the mixed-state properties are governed mainly by point-like disorder. As a result TMI are absent and only a smooth PE is observed. Finally, the critical current density was estimated for both films indirectly from magnetization loop and relaxation measurements (data are not shown here since they are part of

a subsequent publication), and directly by measurements of the $I - V$ characteristics as the ones presented in fig.8 for the Nb-1 film. From those data the critical current density J_c may be straightforwardly estimated for Nb-1 film. Since the dimensions of the specific film are $0.3 \times 0.3 \text{ cm}^2$ and its thickness is 7700 \AA the effective current density is of the order $J_{dc} \simeq 0.1 \text{ kA/cm}^2$. Thus, even in the regime so close to the upper-critical field (for example at $H = 2.3 \text{ kOe} \simeq H_{c2}^{\text{mag}}(8\text{K})$) the critical current density J_c is higher than 0.1 kA/cm^2 (the respective value at low temperatures exceeds 100 kA/cm^2). The respective critical current density of the Nb-2 film is quite lower. All these facts mentioned above suggest that the Nb-1 film is more disordered when compared to Nb-2.

We now discuss the superconducting properties of the films in the regime near the superconducting-normal transition. Interestingly, both films exhibit the same behavior in their residual resistive transitions in the regime $H_{c2}^{\text{mag}}(T) < H < H_{\text{nor}}^{\text{res}}(T)$. This effect could not be related to the bulk properties of the two samples, because it occurs above the bulk upper-critical field line $H_{c2}^{\text{mag}}(T)$. Furthermore, as our XRD and TEM data revealed, the bulk structural properties of the two films differ substantially. Thus, the detected effect could not be related to the resistive properties of the bulk, but probably to the superconducting properties of the surfaces. Thus we conclude that the behavior of the resistive transition above $H_{c2}^{\text{mag}}(T)$ is possibly related to surface superconductivity.

CONCLUSIONS

In summary, we presented magnetic and magneto-transport measurements in films of the isotropic Nb superconductor. Film Nb-1, prepared *under annealing* during the deposition, exhibited TMI and a "SMP" feature in magnetic measurements. In contrast to theoretical suggestions, the first flux jump field H_{fj} is not inversely proportional to the sweep rate of the applied field. TMI are observed up to the limiting temperature $T_o = 7.2 \text{ K}$ where the $H_{fj}(T)$ and $H_{fp}(T)$ lines connect. Interestingly, in the low-temperature regime $T < 6.4 \text{ K}$, the first flux jump field preserves a constant value $H_{fj}(T < 6.4 \text{ K}) = 40 \text{ Oe}$. This is in strong disagreement to theoretical proposals for thin film, or even bulk samples. The comparison of our primary data obtained in film Nb-1 with ancillary data obtained in a bulk sample of MgB_2 , suggest that the TMI exhibit noticeable differences when observed in films or bulk samples. Our TEM and XRD data suggest that in Nb-1 the SMP feature is probably motivated by the interaction of vortices with some kind of correlated disorder existing probably due to the tendency of films that are annealed during deposition to exhibit a columnar growth.

On the other hand, the respective crystallographic data for the less disordered Nb-2 film, which has not

been annealed during deposition, suggest that its mixed-state properties are governed mainly by point-like disorder. As a result Nb-2 exhibited the conventional PE in the vicinity of the upper-critical fields. The end points of the PE exhibit a narrow hysteretic behavior ($\Delta T < 20$ mK), when high magnetic fields are applied. Our results indicate that sharp drops which are usually observed in magnetoresistance data, obtained in low- T_c superconductors, should be interpreted with caution. Such findings should not be directly related to a phase transition of vortex matter. It is only measurements of equilibrium properties that can prove a true phase transition of vortex matter. According to our results, the mechanism of surface superconductivity is probably responsible for the residual part of the magnetoresistance in the region $H_{c2}^{\text{mag}}(T) < H < H_{\text{nor}}^{\text{res}}(T)$. By studying the high field regime in detail, we showed that in contrast to current theoretical treatment the effect is observed not only when the magnetic field is parallel, but also when is normal to the surface of our Nb films.

Finally, let us note that despite the different physical causes, the resulting phase diagrams of vortex matter in our Nb disordered films, have strong analogies to the ones observed in disordered high- T_c superconductors.

This work was supported by the IHP Network "Quantum Magnetic Dots" Contract HPRN-CT-2000-00134 EU.

-
- [1] Blatter G, Feigel'man M V, Geshkenbein V B, Larkin A I and Vinokur V M 1994 *Rev. Mod. Phys.* **66** 1125
- [2] Mikitik G P and Brandt E H 2001 *Phys. Rev. B* **64** 184514
- [3] Menon G I 2002 *Phys. Rev. B* **65** 104527
- [4] Sarkar S *et al.* 2001 *Phys. Rev. B* **64** 144510
- [5] Drulis H *et al.* 1991 *Phys. Rev. B* **44** 4731
- [6] Schmidt M F, Israeloff N E and Goldman A M 1993 *Phys. Rev. Lett.* **70** 2162; *ibid* 1993 *Phys. Rev. B* **48** 3404
- [7] Lynn J W *et al.* 1994 *Phys. Rev. Lett.* **72** 3413; *ibid* 1995 **74**, 1698
- [8] Salem-Sugui S, Friesen M, Alvarenga A D, Gandra F G, Doria M M, and Schilling O F 2002 *Phys. Rev. B* **66** 134521
- [9] Gammel P L *et al.* 1998 *Phys. Rev. Lett.* **80** 833
- [10] Ling X S *et al.* 2001 *Phys. Rev. Lett.* **86** 712
- [11] Forgan E M *et al.* 2002 *Phys. Rev. Lett.* **88** 167003; Forgan E M *et al.* 1995 *Phys. Rev. Lett.* **74** 1697
- [12] Mikitik G P and Brandt E H 2002 *Phys. Rev. Lett.* **89** 259701
- [13] Ling X S, Park S R, McClain B A, Choi S M, Dender D C and Lynn J W 2002 *Phys. Rev. Lett.* **89** 259702
- [14] Esquinazi P, Setzer A, Fuchs D, Kopelevich Y, Zeldov E and Assmann C 1999 *Phys. Rev. B* **60** 12454
- [15] Kopelevich Y and Esquinazi P 1998 *J. Low Temp. Phys.* **113** 1
- [16] Zhukov A A, Kupfer H, Perkins G, Cohen L F, Caplin A D, Klestov S A, Claus H, Voronkova V I, Wolf T and Wühl H 1995 *Phys. Rev. B* **51** 12704
- [17] Stamopoulos D and Pissas M 2001 *Supercond. Sci. Technol.* **14** 844
- [18] Stamopoulos D and Pissas M 2002 *Phys. Rev. B* **65** 134524
- [19] Stamopoulos D, Pissas M and Bondarenko A 2003 *Phys. Rev. B* **66** 214521
- [20] Sun Y P, Hsu Y Y, Lin B N, Luo H M and Ku H C 2000 *Phys. Rev. B* **61** 11301
- [21] Nowak E R, Taylor O W, Liu Li, Jaeger H M and Selinder T I 1997 *Phys. Rev. B* **55** 11702
- [22] Lange M, Bael M J, Bruynseraede Y and Moshchalkov V V 2003 *Phys. Rev. Lett.* **90** 197006
- [23] Martin J I, Velez M, Hoffmann A, Schuller I K and Vicent J L 1999 *Phys. Rev. Lett.* **83** 1022
- [24] Velez M, Jaque D, Martin J I, Montero M I, Schuller I K and Vicent J L 2002 *Phys. Rev. B* **65** 104511
- [25] Stamopoulos D, Pissas M, Karanasos E, Niarchos D and Panagiotopoulos I, accepted for publication in *Phys. Rev. B*
- [26] Finnemore D K, Stromberg T F and Swenson C A 1966 *Phys. Rev.* **149** 231
- [27] Abrikosov A A 1988 *Fundamentals of the Theory of Metals*, (North-Holland)
- [28] Saint-James D and Gennes P G 1963 *Phys. Lett.* **7** 306
- [29] Shantsev D V, Koblishka M R, Galperin Y M, Johansen T H, Pust L and Jirsa M 1999 *Phys. Rev. Lett.* **82** 2947
- [30] The magnetization is estimated when demagnetization corrections are taken into account by claiming that the initial slope of the measured curve should correspond to the Meissner state in which $4\pi |M|$ equals the applied magnetic field. At the same result we arrive if we correct the resulting magnetization by a demagnetization factor N estimated by the approximate formula $N = 1 - (\pi/2)(d/R)$ which holds for the case of a flat disk of thickness d and "diameter" R , when $d \ll R$. [31]
- [31] Fetter A L and Hohenberg P C 1967 *Phys. Rev.* **159** 330
- [32] Mints R G and Brandt E H 1996 *Phys. Rev. B* **54** 12421
- [33] Barkov F L, Shantsev D V, Johansen T H, Goa P E, Kang W N, Kim H J, Choi E M and Lee S I 2003 *Phys. Rev. B* **67** 64513
- [34] Johansen T H, Baziljevich M, Shantsev D V, Goa P E, Galperin Y M, Kang W N, Kim H J, Choi E M, Kim M S and Lee S I 2002 *Europhys. Lett.* **59** 599
- [35] Johansen T H, Baziljevich M, Shantsev D V, Goa P E, Galperin Y M, Kang W N, Kim H J, Choi E M, Kim M S and S.I. Lee 2001 *Supercond. Sci. Technol.* **14** 726
- [36] Zhao Z W *et al.* 2002 *Phys. Rev. B* **65** 64512
- [37] Pissas M and Stamopoulos D (unpublished results).
- [38] Pissas M, Moraitakis E, Stamopoulos D, Papavassiliou G, Psycharis V and Koutandos S 2001 *J. Supercond.* **14** 615
- [39] Wipf S L 1967 *Phys. Rev.* **161** 404; *ibid* 1991 *Cryogenics* **31** 936
- [40] Mints R G and Rakhmanov A L 1981 *Rev. Mod. Phys.* **53** 551
- [41] Grover A K, Ravi Kumar, Malik S K, Chaddah P, Sankaranarayanan V and Subramanian C K 1991 *Phys. Rev. B* **43** 6151
- [42] Welp U, Rydh A, Karapetrov G *et al.* 2003 *Physica C* **385** 154; Welp U, Rydh A, Karapetrov G *et al.* 2003 *Phys. Rev. B* **67** 12505; Rydh A, Welp U, Hiller J M *et al.* cond-mat/0307445 v1
- [43] Shi Z X, Tokunaga M, Tamegai T, Takano Y, Togano K, Kito H and Ihara H 2003 *Phys. Rev. B* **68** 104513

- [44] Swartz P S and Bean C P 1968 *J. Appl. Phys.* **39** 4991
- [45] O'Hara S G, Sellers G J and Anderson A C 1974 *Phys. Rev. B* **10** 2777; Carlson J R and Satterthwaite S B 1970 *Phys. Rev. Lett.* **24** 461
- [46] Brandt E H 1996 *Phys. Rev. B* **54** 4246
- [47] Duran C A, Gammel P L, Miller R E and Bishop D J 1995 *Phys. Rev. B* **52** 75
- [48] Rudnev I A, Antonenko S V, Shantsev D V, Johansen T H and Primenko A E, cond-mat/0211349
- [49] Aranson I, Gurevich A and Vinokur V 2001 *Phys. Rev. Lett.* **87** 067003
- [50] Blanchard S, Klein T, Marcus J, Joumard I, Sulpice A, Szado P, Samuely P, Jansen A G M and Marcenat C 2002 *Phys. Rev. Lett.* **88** 177201
- [51] Kwok W K, Fendrich J, Fleshler S, Welp U, Downey J and Crabtree G W 1994 *Phys. Rev. Lett.* **72** 1092
- [52] Pissas M, Lee S, Yamamoto A and Tajima S 2002 *Phys. Rev. Lett.* **89** 97002
- [53] Pissas M, Stamopoulos D, Lee S and Tajima S, submitted for publication in *Phys. Rev. B*
- [54] Autler S H, Rosenblum E S and Gooen K H 1962 *Phys. Rev. Lett.* **9** 489
- [55] DeSorbo W 1964 *Phys. Rev.* **134** A1119; *ibid* 1964 *Rev. Mod. Phys.* **36** 90
- [56] Tedmon C S, Rose R M and Wulff J 1965 *J. Appl. Phys.* **36** 829
- [57] Tomy C V, Balakrishnan G and Paul D K, 1997 *Physica C* **280** 1; *ibid* 1997 *Phys. Rev. B* **56** 8346
- [58] Ling X S, Berger J E and Proper D E 1998 *Phys. Rev. B* **57** 3249
- [59] Banerjee S S *et al.* 1998 *Phys. Rev. B* **58** 995
- [60] Kupfer H, Wolf T, Lessing C, Zhukov A A, Lancon X, Meier-Hirmer R, Schaner W and Wuhf H 1998 *Phys. Rev. B* **58** 2886; Kupfer H *et al.* 2000 *Physica C* **332** 80
- [61] Blasius T, Niedermayer Ch, Tallon J L, Pooke D M, Golnik A and Bernhard C, 1999 *Phys. Rev. Lett.* **82** 4926
- [62] Giller D *et al.* 1997 *Phys. Rev. Lett.* **79** 2542
- [63] Ertas D and Nelson D R 1996 *Physica C* **272** 79
- [64] Vinokur V *et al.* 1998 *Physica C* **295** 209
- [65] Khaykovich B, Zeldov E, Majer D, Li T W, Kes P H and Konczykowski M 1996 *Phys. Rev. Lett.* **76** 2555
- [66] Giller D, Shaulov A, Yeshurun Y and Giapintzakis J 1999 *Phys. Rev. B* **60** 106
- [67] Kokkalis S, Zhukov A A, Groot P A J, Gagnon R, Taillefer L and Wolf T 2000 *Phys. Rev. B* **61** 3655
- [68] Charalambous M, Chaussy J and Lejay P 1992 *Phys. Rev. B* **45** 5091; *ibid* 1993 *Phys. Rev. Lett.* **71** 436
- [69] Safar H, Gammel P L, Huse D A, Bishop D J, Rice J P and Ginsberg D M 1992 *Phys. Rev. Lett.* **69** 824
- [70] Pradhan A K, Tokunaga M, Shi Z X, Takano Y, Togano K, Kito H, Ihara H and Tamegai T 2002 *Phys. Rev. B* **65** 144513; *ibid* 2001 **64** 212509
- [71] Larkin A I and Ovchinnikov Y N 1979 *J. Low Temp. Phys.* **34** 409
- [72] We estimate the Ginzburg-Landau parameter $\kappa(0) = \lambda(0)/\xi(0)$ from the magnetization measurements. The coherence length $\xi(0) \approx 100 \text{ \AA}$ is estimated from the relation $H_{c2}(T) = \Phi_0/2\pi\xi(T)^2$ by extrapolating the $H_{c2}(T)$ curve down to zero temperature. The zero-temperature penetration depth $\lambda(0)$ may be estimated by the expression $\lambda(0) = \lambda_o \sqrt{\xi_o/2.66l}$. The mean-free path, l may be calculated from the dirty-limit expression $\xi(0) \approx \sqrt{l\xi_o}$ which results in $l \approx 23 \text{ \AA}$, if we assume that $\xi_o = 430 \text{ \AA}$.
- [26] At the end, by assuming $\lambda_o = 350 \text{ \AA}$ [26] we obtain $\lambda(0) \approx 900 \text{ \AA}$. The resulting Ginzburg-Landau parameter is $\kappa(0) \approx 9$.